Our results demonstrate that FFAs lead to steatosis or lipoapoptosis according to the absolute/relative abundance of FFAs, consistent with previous epidemiological data reporting more prevalent NASH in patients with a high intake of saturated fatty acids (64). Our data suggest the potential therapeutic values of the modulation of dietary fatty acids and inhibitors of PLA_2 and GPCR/$G\alpha_i$ in the prevention/treatment of hepatocyte injury in NASH. However, caution is advised for PLA_2 and GPCR/$G\alpha_i$ inhibitors as therapeutic agents, because they could have diverse biological effects on various tissues.

This work was supported by the Nano/Bio Science Program (Grant 2004-00716) and 21C Frontier Functional Proteomics Project from the Korean Ministry of Science and Technology (Grant FPR05C1-160). M-S.L. is an awardee of Science Research Center Grant R01-2005-000-10326-0 from the Korea Science and Engineering Foundation. The authors are grateful to J. B. Kim at Seoul National University for helpful discussions. The authors thank S-D. Rhee and H-G. Cheon at Korea Research Institute of Chemical Technology for their kind provision of mice.

REFERENCES

1. Mulhall, B. P., J. P. Ong, and Z. M. Younossi. 2002. Non-alcoholic fatty liver disease: an overview. *J. Gastroenterol. Hepatol.* **17:** 1136–1143.
2. Matteoni, C. A., Z. M. Younossi, T. Gramlich, N. Boparai, Y. C. Liu, and A. J. McCullough. 1999. Nonalcoholic fatty liver disease: a spectrum of clinical and pathological severity. *Gastroenterology.* **116:** 1413–1419.
3. Schattenberg, J. M., R. Singh, Y. Wang, J. H. Lefkowitch, R. M. Rigoli, P. E. Scherer, and M. Czaja. 2006. JNK1 but not JNK2 promotes the development of steatohepatitis in mice. *Hepatology.* **43:** 163–172.
4. Shimabukuro, M., Y. T. Zhou, M. Levi, and R. H. Unger. 1998. Fatty acid-induced β cell apoptosis: a link between obesity and diabetes. *Proc. Natl. Acad. Sci. USA.* **95:** 2498–2502.
5. Wei, Y., D. Wang, F. Topczewski, and M. J. Pagliassotti. 2006. Saturated fatty acids induce endoplasmic reticulum stress and apoptosis independently of ceramide in liver cells. *Am. J. Physiol. Endocrinol. Metab.* **291:** 275–281.
6. Ji, J., L. Zhang, P. Wang, Y. M. Mu, X. Y. Zhu, Y. Y. Wu, H. Yu, B. Zhang, S. M. Chen, and X. Z. Sun. 2005. Saturated free fatty acid, palmitic acid, induces apoptosis in fetal hepatocytes in culture. *Exp. Toxicol. Pathol.* **56:** 369–376.
7. Feldstein, A. E., N. W. Werneburg, Z. Li, S. F. Bronk, and G. J. Gores. 2006. Bax inhibition protects against free fatty acid-induced lysosomal permeabilization. *Am. J. Physiol. Gastrointest. Liver Physiol.* **290:** 1339–1346.
8. Feldstein, A. E., N. W. Werneburg, A. Canbay, M. E. Guicciardi, S. F. Bronk, R. Rydzewski, L. J. Burgart, and G. J. Gores. 2004. Free fatty acids promote hepatic lipotoxicity by stimulating TNF-alpha expression via a lysosomal pathway. *Hepatology.* **40:** 185–194.
9. Malhi, H., S. F. Bronk, N. W. Werneburg, and G. J. Gores. 2006. Free fatty acids induce JNK-dependent hepatocyte lipoapoptosis. *J. Biol. Chem.* **281:** 12093–12101.
10. Schmid, P. C., E. Deli, and H. H. Schmid. 1995. Generation and remodeling of phospholipid molecular species in rat hepatocytes. *Arch. Biochem. Biophys.* **319:** 168–176.
11. Schmid, P. C., I. Spimrova, and H. H. Schmid. 1995. Incorporation of exogenous fatty acids into molecular species of rat hepatocyte phosphatidylcholine. *Arch. Biochem. Biophys.* **322:** 306–312.
12. Shinzawa, K., and Y. Tsujimoto. 2003. PLA_2 activity is required for nuclear shrinkage in caspase-independent cell death. *J. Cell Biol.* **163:** 1219–1230.
13. Cauwels, A., B. Janssen, A. Waeytens, C. Cuvelier, and P. Brouckaert. 2003. Caspase inhibition causes hyperacute tumor necrosis factor-induced shock via oxidative stress and phospholipase A_2. *Nat. Immunol.* **4:** 387–393.
14. Cnop, M., J. C. Hannaert, A. Hoorens, D. L. Eizirik, and D. G. Pipeleers. 2001. Inverse relationship between cytotoxicity of free fatty acids in pancreatic islet cells and cellular triglyceride accumulation. *Diabetes.* **50:** 1771–1777.
15. Suk, K., S. Kim, Y-H. Kim, K-A. Kim, I. Chang, H. Yagita, M. Shong, and M-S. Lee. 2001. IFNγ/TNFα synergism as the final effector in autoimmune diabetes: a key role for STAT1/IRF-1 in pancreatic β-cell death. *J. Immunol.* **166:** 4481–4489.
16. Cai, J., Y. Zhao, Y. Liu, F. Ye, Z. Song, H. Qin, S. Meng, Y. Chen, R. Zhou, X. Song, et al. 2007. Directed differentiation of human embryonic stem cells into functional hepatic cells. *Hepatology.* **45:** 1229–1239.
17. Yan, J. J., J. S. Jung, J. E. Lee, J. Lee, S. O. Huh, H. S. Kim, K. C. Jung, J. Y. Cho, J. S. Nam, H. W. Suh, et al. 2004. Therapeutic effects of lysophosphatidylcholine in experimental sepsis. *Nat. Med.* **10:** 161–167.
18. Winitz, S., S. K. Gupta, N-X. Qian, L. E. Heasley, R. A. Nemenoff, and G. L. Johnson. 1994. Expression of a mutant $Gi_3\alpha$ subunit inhibits ATP and thrombin stimulation of cytoplasmic phospholipase A_2-mediated arachidonic acid release independent of Ca^{2+} and mitogen-activated protein kinase regulation. *J. Biol. Chem.* **269:** 1889–1895.
19. Polyak, K., Y. Xia, J. L. Zweier, K. W. Kinzler, and B. Vogelstein. 1997. A model for p53-induced apoptosis. *Nature.* **389:** 300–305.
20. Chang, I., N. Cho, S. Kim, J. Y. Kim, E. Kim, J-E. Woo, J. H. Nam, S. J. Kim, and M-S. Lee. 2004. Role of calcium in pancreatic islet cell death by IFNγ/TNFα. *J. Immunol.* **172:** 7008–7014.
21. Lee, K. W., J. B. Park, J. J. Yoon, J. H. Lee, S. Y. Kim, H. J. Jung, S. K. Lee, S. J. Kim, H. H. Lee, D. S. Lee, et al. 2004. The viability and function of cryopreserved hepatocyte spheroids with different cryopreservation solutions. *Transplant. Proc.* **36:** 2462–2463.
22. Tong, J. Z., O. Bernard, and F. Alvarez. 1990. Long-term culture of rat liver cell spheroids in hormonally defined media. *Exp. Cell Res.* **189:** 87–92.
23. Nakagawa, T., S. Shimizu, T. Watanabe, O. Yamaguchi, K. Otsu, H. Yamagata, H. Inohara, T. Kubo, and Y. Tsujimoto. 2005. Cyclophilin D-dependent mitochondrial permeability transition regulates some necrotic but not apoptotic cell death. *Nature.* **434:** 652–658.
24. Smani, T., S. I. Zakharov, P. Csutora, E. Leno, E. S. Trepakova, and V. M. Bolotina. 2004. A novel mechanism for the store-operated calcium influx pathway. *Nat. Cell Biol.* **6:** 113–120.
25. Joshi, S. S., C. A. Kuszynski, M. Bakchi, and D. Bagchi. 2000. Chemopreventive effects of grape seed proanthocyanidin extract of Chang liver cells. *Toxicology.* **155:** 83–90.
26. Obeid, L. M., C. M. Linardic, L. A. Karolak, and Y. A. Hannun. 1993. Programmed cell death induced by ceramide. *Science.* **259:** 1769–1771.
27. Knoll, L. J., O. F. Schall, I. Suzuki, G. W. Gokel, and J. I. Gordon. 1995. Comparison of the reactivity of tetradecanoic acids, a triacsin, and unsaturated oximes with four purified *Saccharomyces cerevisiae* fatty acid activation proteins. *J. Biol. Chem.* **270:** 20090–20097.
28. Tonnetti, L., M. C. Veri, E. Bonvini, and L. D'Adamio. 1999. A role for neutral sphingomyelinase-mediated ceramide production in T cell receptor-induced apoptosis and mitogen-activated protein kinase-mediated signal transduction. *J. Exp. Med.* **189:** 1581–1589.
29. Ogretmen, B., B. J. Pettus, M. J. Rossi, R. Wood, J. Usta, Z. Szulc, A. Bielawska, L. M. Obeid, and Y. A. Hannun. 2002. Biochemical mechanisms of the generation of endogenous long chain ceramide in response to exogenous short chain ceramide in the A549 human lung adenocarcinoma cell line. *J. Biol. Chem.* **277:** 12960–12969.
30. Eitel, K., H. Staiger, J. Rieger, H. Mischak, H. Brandhorst, M. D. Brendel, R. G. Bretzel, H. U. Haring, and M. Kellerer. 2003. Protein kinase C delta activation and translocation to the nucleus are required for fatty acid-induced apoptosis of insulin-secreting cells. *Diabetes.* **52:** 991–997.
31. Finney, R. E., E. Nudelman, T. White, S. Bursten, P. Klein, L. L. Leer, N. Wang, D. Waggoner, J. W. Singler, and R. A. Lewis. 2000. Pharmacological inhibition of phosphatidylcholine biosynthesis is associated with induction of phosphatidylinositol accumulation and cytolysis of neoplastic lines. *Cancer Res.* **60:** 5204–5213.
32. Balsinde, J., and E. A. Dennis. 1996. Bromoenol lactone inhibits magnesium-dependent phosphatidate phosphohydrolase and blocks triacylglycerol biosynthesis in mouse P388D1 macrophages. *J. Biol. Chem.* **271:** 31937–31941.
33. Kabarowski, J. H. S., K. Zhu, L. Q. Le, O. N. Witte, and Y. Xu. 2001.

Lysophosphatidylcholine as a ligand for the immunoregulatory receptor G2A. *Science.* **293:** 702–705.
34. Zhu, K., L. B. Baudhuin, G. Hong, F. S. Williams, K. L. Cristina, J. H. S. Kaharowski, O. N. Witte, and Y. Xu. 2001. Sphingosylphosphorylcholine and lysophosphatidylcholine are ligands for the G protein-coupled receptor GPR4. *J. Biol. Chem.* **276:** 41325–41335.
35. Goonesinghe, A., E. S. Mundy, M. Smith, R. Khosravi-Far, J. C. Martinou, and M. D. Esposti. 2005. Pro-apoptotic Bid induces membrane perturbation by inserting selected lysolipids into the bilayer. *Biochem. J.* **387:** 109–118.
36. Fang, X., S. Gibson, M. Flowers, T. Furui, R. C. Bast, and G. B. Mills. 1997. Lysophosphatidylcholine stimulates activator protein 1 and the c-Jun N-terminal kinase activity. *J. Biol. Chem.* **272:** 13688–13689.
37. Listenberger, L. L., X. Han, S. E. Lewis, S. Cases, R. V. Farese, D. S. Ory, and J. E. Schaffer. 2003. Triglyceride accumulation protects against fatty acid-induced lipotoxicity. *Proc. Natl. Acad. Sci. USA.* **100:** 3077–3082.
38. Ishak, K., A. Baptista, L. Bianchi, F. Callea, J. D. Groote, F. Gudat, H. Denk, V. Desmet, G. Korb, R. N. M. MacSween, et al. 1995. Histological grading and staging of chronic hepatitis. *J. Hepatol.* **22:** 696–699.
39. Lee, J-S., and S. S. Thorgeirsson. 2002. Functional and genomic implications of global gene expression profiles in cell lines from human hepatocellular cancer. *Hepatology.* **35:** 1134–1143.
40. Fernandez-Martiniz, A., B. Molla, R. Mayoral, L. Boaca, M. Casado, and P. Martin-Sanz. 2006. Cyclo-oxygenase 2 expression impairs serum-withdrawal-induced apoptosis in liver cells. *Biochem. J.* **398:** 371–380.
41. Paumen, M. B., Y. Ishida, M. Muramatsu, M. Yamamoto, and T. Honjo. 1997. Inhibition of carnitine palmitoyltransferase I augments sphingolipid synthesis and palmitate-induced apoptosis. *J. Biol. Chem.* **272:** 3324–3329.
42. Listenberger, L. L., D. S. Ory, and J. E. Shaffer. 2001. Palmitate-induced apoptosis can occur through a ceramide-independent pathway. *J. Biol. Chem.* **276:** 14890–14895.
43. Hardy, S., W. El-Assaad, E. Przybytkowski, E. Joly, M. Prentki, and Y. Langelier. 2003. Saturated fatty acid-induced apoptosis in MDA-MB-231 breast cancer cells. *J. Biol. Chem.* **278:** 31861–31870.
44. Takahashi, M., H. Okazaki, Y. Ogata, K. Takeuchi, U. Ikeda, and K. Shimada. 2002. Lysophosphatidylcholine induces apoptosis in human endothelial cells through a p38-mitogen-activated protein kinase-dependent mechanism. *Atherosclerosis.* **161:** 387–394.
45. Kinsey, G. R., B. S. Cummings, C. S. Beckett, G. Saavedra, W. Zhang, J. McHowat, and R. G. Schnellmann. 2005. Identification and distribution of endoplasmic reticulum iPLA$_2$. *Biochem. Biophys. Res. Commun.* **327:** 287–293.
46. Jenkins, C. M., D. J. Mancuso, W. Yan, H. F. Sims, B. Gibson, and R. W. Gross. 2004. Identification, cloning, expression, and purification of three novel human calcium-independent phospholipase A$_2$ family members possessing triacylglycerol lipase and acylglycerol transacylase activities. *J. Biol. Chem.* **279:** 48968–48975.
47. Williams, S. D., and R. A. Gottlieb. 2002. Inhibition of mitochondrial calcium-independent phospholipase A$_2$ (iPLA$_2$) attenuates mitochondrial phospholipid loss and is cardioprotective. *Biochem. J.* **362:** 23–32.
48. Yellaturu, C. R., and G. N. Rao. 2003. A requirement for calcium-independent phospholipase A$_2$ in thrombin-induced arachidonic acid release and growth in vascular smooth muscle cells. *J. Biol. Chem.* **278:** 43831–43837.
49. Martinez, J., and J. J. Moreno. 2001. Role of Ca^{2+}-independent phospholipase A$_2$ on arachidonic acid release induced by reactive oxygen species. *Arch. Biochem. Biophys.* **392:** 257–262.
50. Masamune, A., Y. Sakai, A. Satoh, M. Fujita, M. Yoshida, and T. Shimosegawa. 2001. Lysophosphatidylcholine induces apoptosis in AR42J cells. *Pancreas.* **22:** 75–83.
51. Philips, G. B., and J. T. Dodge. 1967. Composition of phospholipids and of phospholipid fatty acids of human plasma. *J. Lipid Res.* **8:** 676–681.
52. Okita, M., D. C. Gaudette, G. B. Mills, and B. J. Holub. 1997. Elevated levels and altered fatty acid composition of plasma lysophosphatidylcholine (lysoPC) in ovarian cancer patients. *Int. J. Cancer.* **71:** 31–34.
53. Ostrander, D. B., G. C. Sparagna, A. A. Amoscato, J. B. McMillin, and W. Dowhan. 2001. Decreased cardiolipin synthesis corresponds with cytochrome c release in palmitate-induced cardiomyocyte apoptosis. *J. Biol. Chem.* **276:** 38061–38067.
54. Solinas, G., W. Naugler, F. Galimi, M-S. Lee, and M. Karin. 2006. Saturated fatty acids inhibit induction of insulin gene transcription via JNK-mediated phosphorylation of insulin receptor substrates. *Proc. Natl. Acad. Sci. USA.* **103:** 16454–16459.
55. Lin, P., and R. D. Ye. 2003. The lysophospholipid receptor G2A activates a specific combination of G proteins and promotes apoptosis. *J. Biol. Chem.* **278:** 14379–14386.
56. Hama, K., J. Aoki, M. Fukaya, Y. Kishi, T. Sakai, R. Suzuki, H. Ohta, T. Yamori, M. Watanabe, J. Chun, et al. 2004. Lysophosphatidic acid and autotaxin stimulate cell motility of neoplastic and non-neoplastic cells through LPA1. *J. Biol. Chem.* **279:** 17634–17639.
57. Umezu-Goto, M., Y. Kishi, A. Taira, K. Hama, N. Dohmae, K. Takio, T. Yamori, G. B. Mills, K. Inoue, J. Aoki, et al. 2002. Autotaxin has lysophospholipase D activity leading to tumor cell growth and motility by lysophosphatidic acid production. *J. Cell Biol.* **158:** 227–233.
58. van den Besselaar, A. M. H. P., B. de Kruijff, H. van den Bosch, and L. L. M. van Deenen. 1979. Transverse distribution and movement of lysophosphatidylcholine in sarcoplasmic reticulum membranes as determined by ^{13}C-NMR and lysophospholipase. *Biochim. Biophys. Acta.* **555:** 193–199.
59. Xie, Y., T. C. Gibbs, and K. E. Meier. 2002. Lysophosphatidic acid as an autocrine and paracrine mediator. *Biochim. Biophys. Acta.* **1582:** 270–281.
60. Xu, F. Y., W. A. Taylor, and G. M. Match. 1998. Lysophosphatidylcholine inhibits cardiolipin biosynthesis in H9c2 cardiac myoblast cells. *Arch. Biochem. Biophys.* **349:** 341–348.
61. Ott, M., J. D. Robertson, V. Gogvadze, B. Zhivotovsky, and S. Orrenius. 2002. Cytochrome *c* release from mitochondria proceeds by a two-step process. *Proc. Natl. Acad. Sci. USA.* **99:** 1259–1263.
62. Ryden, M., E. Arvidsson, L. Blomqvist, L. Perbeck, A. Dicker, and P. Arner. 2004. Targets for TNF-α-induced lipolysis in human adipocytes. *Biochem. Biophys. Res. Commun.* **318:** 168–175.
63. Yang, S. Q., H. Z. Lin, M. D. Lane, M. Clemens, and A. M. Diehl. 1997. Obesity increases sensitivity to endotoxin liver injury: implications for the pathogenesis of steatohepatitis. *Proc. Natl. Acad. Sci. USA.* **94:** 2557–2562.
64. Musso, G., R. Gambino, F. De Michieli, M. Cassader, M. Rizzetto, M. Durazzo, E. Faga, B. Silli, and G. Pagano. 2003. Dietary habits and their relations to insulin resistance and postprandial lipemia in nonalcoholic steatohepatitis. *Hepatology.* **37:** 909–916.

Am J Physiol Endocrinol Metab 295: E1349–E1357, 2008.
First published October 7, 2008; doi:10.1152/ajpendo.90704.2008.

Bis deficiency results in early lethality with metabolic deterioration and involution of spleen and thymus

Dong-Ye Youn,[1]* Dong-Hyoung Lee,[1]* Mi-Hyun Lim,[1] Jung-Sook Yoon,[2] Ji Hee Lim,[2] Seung Eun Jung,[1] Chung Eun Yeum,[3] Cheol Whee Park,[2] Ho-Joong Youn,[2] Jae-Seon Lee,[4] Seong-Beom Lee,[3] Masahito Ikawa,[5] Masaru Okabe,[5] Yoshihide Tsujimoto,[6,7] and Jeong-Hwa Lee[1]

[1]*Department of Biochemistry,* [2]*Department of Internal Medicine, and* [3]*Department of Pathology, College of Medicine, Catholic University of Korea and* [4]*Division of Radiation Cancer Research, Korea Institute of Radiological and Medical Science, Seoul, Korea; and* [5]*Genome Information Research Center, Research Institute for Microbial Diseases, Osaka University,* [6]*Department of Medical Genetics, Laboratory of Molecular Genetics, Osaka University Medical School, and* [7]*Solution-Oriented Research for Science and Technology, Japan Science and Technology Agency, Osaka, Japan*

Submitted 18 August 2008; accepted in final form 25 September 2008

Youn DY, Lee DH, Lim MH, Yoon JS, Lim JH, Jung SE, Yeum CE, Park CW, Youn HJ, Lee JS, Lee SB, Ikawa M, Okabe M, Tsujimoto Y, Lee JH. Bis deficiency results in early lethality with metabolic deterioration and involution of spleen and thymus. *Am J Physiol Endocrinol Metab* 295: E1349–E1357, 2008. First published October 7, 2008; doi:10.1152/ajpendo.90704.2008.— Bcl-2 interacting cell death suppressor (Bis), also known as Bag3 or CAIR-1, is involved in antistress and antiapoptotic pathways. In addition to Bcl-2, Bis binds to several proteins, suggesting it has diverse functions in normal and pathological conditions. To better define the physiological function of Bis in vivo, we developed *bis*-deficient mice with a *cre-loxP* system. Targeted disruption of exon 4 of the *bis* gene was demonstrated by Southern blotting and PCR, and Western blotting showed that no intact or truncated Bis protein was synthesized in $bis^{-/-}$ mice. While heterozygotes were fertile and appeared normal, Bis-deficient mice showed growth retardation and died by 3 wk after birth. The relative weight of the thymus and spleen was reduced and the total numbers of white blood cells, splenocytes, and thymocytes were significantly reduced compared with wild-type littermates. Serum profiles indicated significant hypoglycemia as well as decrease in triglyceride and cholesterol levels. Expression profiles of metabolic genes indicated that gluconeogenesis and β-oxidation are activated in the liver of $bis^{-/-}$ mice. This activation, as well as a decrease in peripheral fat and an induction of fatty liver, appears to be an adaptive response to hypoglycemia. Our study reveals that the absence of Bis has considerable influences on postnatal growth and survival, possibly due to a nutritional impairment.

bis; knockout; hypoglycemia

THE BCL-2 INTERACTING DEATH SUPPRESSOR (*bis*) gene has been identified as encoding a Bcl-2 binding protein in protein interaction techniques (18). Bis has also been reported as Bag3 and CAIR-1, which bind to heat shock protein (HSP)70 and PLC-γ, respectively (7, 33). The ability of Bis to bind to several proteins suggests that it has distinct functions depending on its cellular environment. A possible role for Bis in modulating cell death was revealed in in vitro DNA transfection experiments in which Bis was shown to significantly enhance the antiapoptotic function of Bcl-2 (18). Supporting this, Bis has also been shown to be specifically expressed or overexpressed in several cancers, including pancreatic cancer, thyroid carcinoma, and some leukemia (1, 5, 21, 27, 28). Furthermore, the downmodulation of Bis results in an increased susceptibility for the induction of apoptosis in cancer cells (1, 5, 26). Bis has been also proposed as an antistress protein, based on the upregulation of its expression, concomitant with HSP70, in cells exposed to stressful stimuli such as heat shock or heavy metals (21, 23). In addition to the stressful conditions given for cellular levels, the expression of Bis is significantly upregulated in several in vivo disease models such as stroke and seizure models (19, 20, 31). Moreover, Bis is robustly expressed in reactive astrocytes in areas of gliosis in the brain of human immunodeficiency virus (HIV) encephalopathy patients (29). Light damage also increases the expression of Bis in the mouse retina (4). These results suggest that the expression of Bis may be induced to protect cells from stressful conditions, but the persistent and/or uncontrolled expression of Bis may contribute to the progression of cancer.

In addition to its possible role as a stress- or survival-related protein, Bis has been implicated to have other cellular functions. Overexpression of Bis promotes the differentiation of human promyelocytic cells and cell cycle arrest (32). Roles for Bis in cell adhesion and migration have been recently reported by separate groups, although their results differ: in one study overexpression of Bis is shown to inhibit the migration and adhesion of breast cancer cell lines, whereas in the other study *bis*-deficient fibroblasts have reduced motility and delayed formation of focal adhesion complex (12, 14). These results suggest that complex mechanisms are involved in the regulation of cellular motility by Bis. Furthermore, cytoplasmic Bis protein modulates the transcription of the HIV-1 gene and the replication of the varicella-zoster virus (15, 29). Therefore, it appears that Bis exerts diverse functions in pathophysiological conditions in vivo, which may be partly ascribed to its ability to interact with several known and yet to be identified proteins.

To better define the function of Bis in vivo, we developed *bis*-deficient mice with a *cre-loxP* system targeting exon 4. Here we show that disruption of exon 4 of the *bis* gene by homologous recombination led to a complete inhibition of Bis protein synthesis, which resulted in serious hypoglycemia, a fatty liver, and 100% lethality before 3 wk of age. Bis-deficient mice also exhibited a significant involution of the spleen and thymus. Our results are inconsistent with a previous study in

* D.-Y. Youn and D.-H. Lee contributed equally to this work.

Address for reprint requests and other correspondence: J.-H. Lee, 505 Banpo-Dong, Seocho-gu, Seoul 137-701, Korea (e-mail: leejh@catholic.ac.kr).

The costs of publication of this article were defrayed in part by the payment of page charges. The article must therefore be hereby marked "*advertisement*" in accordance with 18 U.S.C. Section 1734 solely to indicate this fact.

which retrovirus-targeted deletion of the *bis* gene resulted in massive degeneration of myofibrils with apoptotic features in heart and skeletal muscles and no abnormalities in other organs (10). Possible explanations for the differences observed in *bis*-deficient mice in the previously published study and the present study are discussed below.

METHODS

Construction of targeting vector and generation of bis-mutant mice. A 6,018-bp genomic clone that includes coding exons 3 and 4 of the *bis* gene (nucleotides 17173-23356 from the start codon) was cloned from D3 mouse embryonic stem (ES) cells as the long arm and introduced into a pMulti-ND 1.0 vector with *Pme*I and *Pac*I sites (11). The *loxP* sequences were inserted into an *Eco*RV site located between exon 3 and exon 4. For homologous recombination, the downstream short arm spanning nucleotides 23357-27370 was also cloned and introduced into a *Not*I site of a pMulti vector. The resulting *Pme*I-digested targeting vector was electroporated into D3 ES cells derived from 129Sv and screened for neomycin resistance. Of 98 neomycin-resistant clones, four clones were shown to have the desired homologous recombination as determined by Southern blotting with two different probes for the 5′ and 3′ regions external to the targeting vector and one probe for the neomycin sequences. Four homologous recombinant ES clones were independently injected into C57B6 blastocysts to generate chimeric mice. Male chimera derived from one ES clone transmitted the recombinant allele to the next generation. To generate heterozygous mutants with deletion of exon 4 of the *bis* gene on one chromosome, the germ line-transmitted male mice were mated with *CAG-cre* C57B6 females.

All research procedures involving animals were performed in accordance with the Laboratory Animals Welfare Act, the *Guide for the Care and Use of Laboratory Animals*, and the Guidelines and Policies for Rodent Experiments provided by the Institutional Animal Care and Use Committee (IACUC) at the College of Medicine, Catholic University of Korea and were reviewed and approved by the IACUC.

Southern blotting and allele-specific genomic PCR. Genomic DNA extracted from wild-type or *bis*-mutant mice livers was digested with *Bam*HI enzyme and electrophoresed through 0.8% agarose. After transfer onto nylon membrane by capillary blotting, the membrane was hybridized with a digoxigenin (DIG)-labeled specific DNA probe and then immunodetected with alkaline phosphatase-conjugated anti-DIG antibody and a chemiluminescent substrate (Roche Applied Science, Mannheim, Germany) as described previously (17). The following primers were used to incorporate DIG-11 dUTP for the DNA probes: 5′-TGA GGT AAG AAG AGA CCC AGA GAC (forward primer) and 5′-TAC AGA CGT AGG AAA CAC ATC TCC (reverse primer).

PCR reactions were also performed to detect the truncated *bis* allele in genomic DNA with two sets of primers, 5′-TGA GAG CCA GCA TGC TGT TTC ATT and 5′-TGG CCC TCA GGG GAC AAC CTG CAG designed to amplify a region of 500 bp in the wild-type allele and 5′-CTT TCA AGG ATT TAA CTT ATC TGA CCA and 5′-ACA GCA AGC ATA TTC CTC TAC CTA AG to amplify a 3,003-bp product in the wild-type allele and a 1,043-bp product in the post-*cre* allele. PCR products were electrophoresed on a 1.5% agarose gel and visualized with ethidium bromide staining.

Western blotting. Proteins from various tissues of wild-type or *bis*-mutant mice were prepared and Western blotting was performed as described previously (17). To analyze Bis expression, the blotted membranes were incubated with polyclonal antibodies against the COOH-terminal half of human Bis (306-575 aa) (18) or against whole human Bis (Abnova, Taiwan, Taipei). Polyclonal antibodies raised in rabbit against the NH_2-terminal of human Bis (48-63 aa) (Peptron, Daejeon, Korea) were also used to detect smaller truncated Bis proteins. Antibodies for HSP70 and Bcl-2 were purchased from BD Biosciences (San Jose, CA) and Santa Cruz Biotechnology (Santa Cruz, CA), respectively.

Complete blood count and assay of metabolites in blood and liver. The complete blood count was determined with a Hemavet 850 automated hematologic analyzer (CDC Technologies, Oxford, CT). The concentration of glucose in the blood was determined by Hemocue Glucose 201+ (Hemocue, Angelholm, Sweden). Plasma concentration of insulin was measured with a mouse insulin enzyme-linked immunoabsorbent assay kit (Linco Research, Erie, PA). Measurements of triglyceride, free fatty acid, and cholesterol in the serum and in the liver were performed with the Triglyceride E-test, NEFA-HR (2), and Labassay Cholesterol, respectively (Wako Pure Chemical Industries, Osaka, Japan).

Histological analysis. Paraffin sections (10 μm) from various organs were processed for hematoxylin and eosin (H & E) staining. Frozen liver sections (6 μm) were fixed with 10% formalin, stained with 0.5% Oil Red O, and counterstained with Mayer's hematoxylin. To examine the state of apoptosis in situ in muscles, a terminal deoxynucleotidyl transferase-mediated dUTP nick end labeling (TUNEL) assay was also performed with the ApopTag Peroxidase In Situ Apoptosis Detection Kit S7100 (Chemicon, Temecula, CA). Specimens were examined under a light microscope (Axioskop40, Carl Zeiss, Gottingen, Germany). For electron microscopy, the tissue samples were fixed with 2.5% glutaraldehyde for 1 h. After fixation, the samples were postfixed in 1% O_sO_4, dehydrated in ethanol, and embedded in Epon 812 (Polysciences, Warrington, PA). Ultrathin sections were contrasted with uranyl acetate and lead citrate. Sections were examined in a JEM 1010 CX transmission electron microscope (JEOL, Akishima, Japan).

RNA extraction and quantitative real-time PCR. Total RNA from liver was isolated with RNA-Bee (Tel-Test, Friendswood, TX). cDNA was synthesized from 2 μg of total RNA with AccuPower Cycle Script (dN6) (Bioneer, Daejeon, Korea). mRNA levels of genes involved in glucose and lipid metabolism were measured by quantitative real-time PCR using a cDNA template and appropriate primers as previously described (Refs. 9, 25, 34; Supplemental Table S1).[1] Quantitative real-time PCR was performed with the IQ5 Real Time PCR detection System (Bio-Rad Laboratories, Hercules, CA) and iQ TM SYBR Green Supermix (Bio-Rad Laboratories). Relative levels of PCR products were determined after normalizing to an endogenous cyclophilin control.

Statistical analysis. The number of mice in each experimental group is indicated in Figs. 2 and 3. A two-tailed Student's *t*-test was used to calculate *P* values. All values are presented as means ± SE. Differences were considered significant if $P < 0.05$.

RESULTS

Targeting the bis gene and generation of bis-mutant mice. The coding region of mouse *bis* consists of four exons. The 315-amino acid peptide encoded by exon 4 includes the bag domain and a proline-rich region, which are required for the regulation of HSP70 chaperone activity and cellular motility, respectively (14, 33). To disrupt exon 4, we generated a targeting vector in which exon 4 was bracketed by *loxP* sites as shown in Fig. 1*A*. The germ line-transmitted male mice were obtained and mated with *CAG-cre* C57B6 females as described in METHODS. The resulting heterozygous male *bis* mutants were backcrossed into C57B6 females for more than eight generations to minimize the contribution of the 129Sv genetic background of ES cells on the phenotype of *bis* mutants. Male and female *bis* heterozygotes were interbred to generate homozygous mice. In $bis^{-/-}$ mice, the *loxP* sites and the intervening

[1] The online version of this article contains supplemental material.

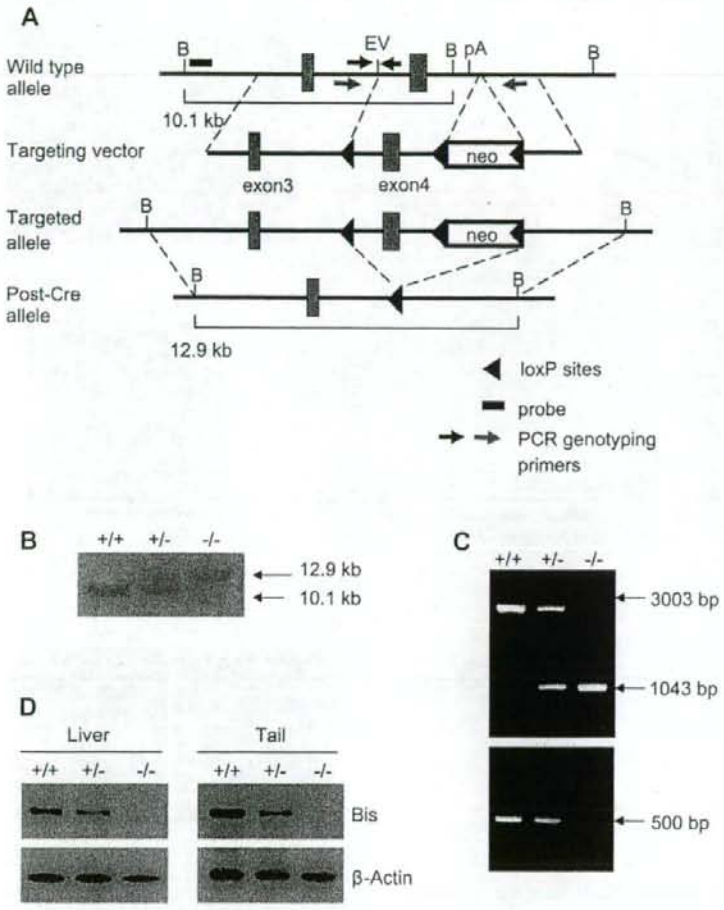

Fig. 1. Targeted disruption of the *bis* gene. *A*: schematic representation of a part of the *bis* genomic locus, targeting vector, and mutant allele. The targeting vector includes the 5′ long arm, the neomycin-resistant gene (*neo*), and the 3′ short arm for homologous recombination. Exon 4, as well as *neo*, was flanked by *loxP* sequences, shown as arrowheads. The sizes of *Bam*HI DNA fragments are indicated beneath the wild-type allele and post-*cre* allele. The 5′ external probe used for Southern blotting is shown as a black square. The small black and gray arrows indicate the locations of the primers used for genotyping. B, *Bam*HI; EV, *Eco*RV; pA, poly A. *B*: Southern blot analysis. Genomic DNA (10 μg) was extracted from liver of mice of the indicated *bis* genotypes. Hybridization of genomic DNA with the external probe, shown in *A*, revealed a 10.1-kb *Bam*HI fragment for wild-type allele and a 12.9-kb *Bam*HI fragment for knockout allele, corresponding to the deletion of a *Bam*HI site and exon 4 by *Cre* excision. *C*: PCR analysis. Genomic DNA was isolated from mouse tails, and PCR screening was performed with 2 pairs of primers, indicated in *A*. A pair of primers (gray arrows in *A*) were designed to produce a 3,003-bp product from the wild-type allele and a 1,043-bp product from the post-*cre* allele. Another pair of primers (black arrows in *A*) failed to amplify a 500-bp product in homozygous $bis^{-/-}$ mice because of the deletion of a section of DNA that contained the reverse primer site. *D*: Western blotting using whole protein extracts from liver and tail revealed that there is no intact Bis protein in $bis^{-/-}$ mice.

DNA, including a *Bam*HI site, were deleted, generating a 12.9-kb fragment of *Bam*HI compared with a 10.1-kb fragment in $bis^{+/+}$ mice, as shown in a Southern blot using genomic DNA extracted from the tail (Fig. 1*B*). PCR analysis using two pairs of primers, upstream and downstream of either the first *loxP* site or all three *loxP* sites, also confirmed the elimination of the DNA fragment flanked by the *loxP* sites (Fig. 1*C*). Expression of the 80-kDa Bis protein was reduced in $bis^{+/-}$ heterozygous and undetectable in $bis^{-/-}$ homozygous mouse liver tissues in a Western blot with Bis-specific antibody against the COOH terminus of Bis (Fig. 1*D*). Neither anti-Bis antibodies raised against whole peptides of Bis nor anti-Bis antibodies specific for its NH_2 terminus showed any smaller size of Bis protein products in heterozygous and homozygous tissues, excluding the possibility of the presence of truncated Bis protein composed of exon 1 from exon 3 (Supplemental Fig. S1). Therefore, disruption of exon 4 of the *bis* gene resulted in the complete inhibition of synthesis of both intact Bis protein and aberrant forms of Bis.

General characteristics of $bis^{-/-}$ mice. The $bis^{-/-}$ offspring were born roughly in a Mendelian ratio: 67 $bis^{-/-}$ homozygous, 135 $bis^{+/-}$ heterozygous, and 75 $bis^{+/+}$ wild type. While $bis^{+/-}$ heterozygous mice appeared normal and were fertile, all $bis^{-/-}$ homozygous mice died before 3 wk of age. As shown in Fig. 2*A*, the difference in body weight between homozygous $bis^{-/-}$ and both heterozygous and wild-type mice was imperceptible at birth but became noticeable within 1 wk after birth and obvious until 12–13 days after birth. Thereafter, the $bis^{-/-}$ mice failed to gain weight and began to gradually lose body weight before they died. Apparently, the thymus and spleen of $bis^{-/-}$ mice shrank dramatically to 51% and 36% of wild type, respectively, in terms of weight per total body weight at 16 days after birth (Fig. 2, *C* and *D*). The involution of spleen in *bis*-deficient mice appeared before that of thymus, showing a reduction of relative weight to 50% of wild type at 14 days after birth but no reduction of thymus (Fig. 2*E*). In addition, the external surface of livers from $bis^{-/-}$ mice, which were 80% of the relative weight of wild-type livers, appeared pale (Fig. 2, *C*

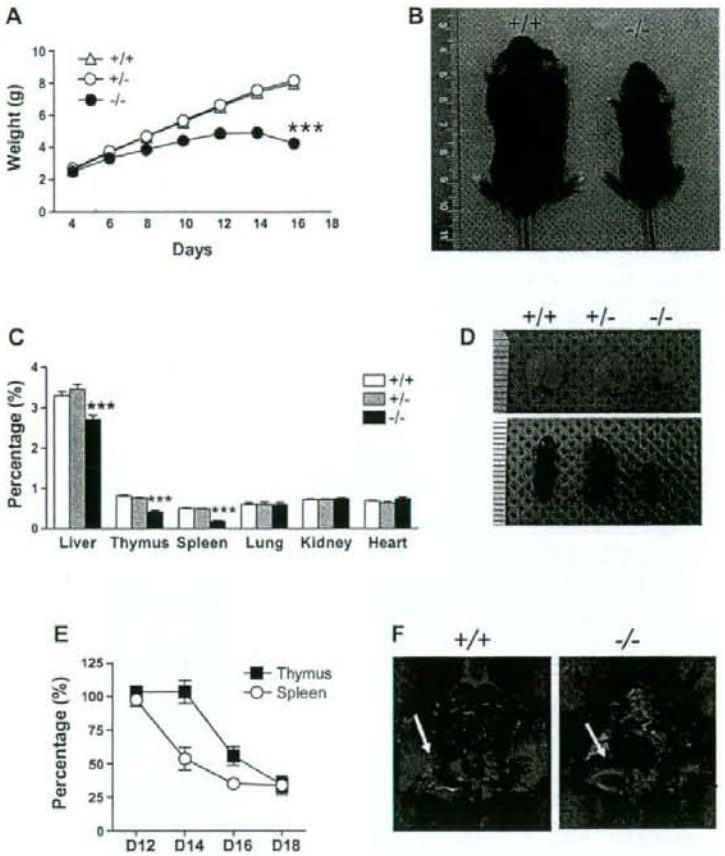

Fig. 2. Characterization of *bis*-deficient mice. *A*: growth of wild-type and $bis^{-/-}$ mice. Offspring generated from heterozygous intercrosses of $bis^{+/-}$ mice were weighed at 2-day intervals from 4 days until 16 days after birth. [n = 46 for wild-type (+/+), 104 for $bis^{+/-}$, 36 for $bis^{-/-}$]. ***$P < 0.001$, compared with wild-type littermates. *B*: representative picture showing significant growth retardation of a $bis^{-/-}$ mouse compared with a wild-type littermate at 16 days of age. *C*: relative weight of each organ to total body weight as shown as %. The ratios of thymus and spleen weight to total body weight in homozygous $bis^{-/-}$ mice were significantly decreased compared with those in wild-type and heterozygous mice older than 16 days of age (n = 15 for $^{+/+}$, 12 for $bis^{+/-}$, 16 for $bis^{-/-}$). ***$P < 0.001$, compared with wild-type littermates. *D*: representative morphology of thymus (*top*) and spleen (*bottom*) at 16 days of age showing notable reduction in size in *bis*-deficient mice. *E*: the decreased size of the thymus and spleen in *bis*-deficient mice was not obvious until age 12 days; thereafter, shrinkage of the spleen occurred before that of the thymus. The relative weight of the thymus and the spleen in $bis^{-/-}$ mice was compared with that of wild-type littermates, and the ratio is shown as %. The data are means ± SE. The number of animals measured each day is 4, 6, 8, and 5 for days (D)12, 14, 16, and 18, respectively. *F*: reduction of subcutaneous fat (white arrow) and periepididymal fat (black arrow) in a male *bis*-deficient mouse at 16 days of age compared with a wild-type male littermate.

and *F*). Notably, the subcutaneous fat and the perigonadal fat were severely reduced in $bis^{-/-}$ mice compared with wild-type mice at day 16 (Fig. 2*F*).

Decreased number of thymocytes, splenocytes, and leukocytes in peripheral blood of bis-deficient mice. As predicted from the reduced size of the thymus and spleen of *bis*-deficient mice, the number of splenocytes and thymocytes was significantly decreased, about one-tenth and one-fifth compared with wild type in the spleen and thymus, respectively, at ≥16 days of age (Table 1). The *bis*-deficient mice also had a >50% decrease in the number of total peripheral leukocytes, but the proportion of neutrophils and lymphocytes was not significantly different from that in wild-type littermates (Table 1). The difference in the number of red blood cells and platelets in *bis*-deficient and wild-type mice was insignificant.

Bis deficiency caused hypoglycemia and hepatic steatosis. The reduction in perigonadal and subcutaneous fat in $bis^{-/-}$ mice suggested that the mice suffered from malnutrition and led us to inspect the metabolic parameters in the serum. As shown in Table 2, serum glucose levels were decreased to one-third the levels of wild type in $bis^{-/-}$ mice. Insulin levels were also lower in *bis*-deficient mice than in $bis^{+/+}$ mice, showing that the hypoglycemia observed in the $bis^{-/-}$ mice was not due to high levels of insulin. Total cholesterol and triglyceride levels were also significantly decreased in *bis*-deficient mice, 60% and 26% of those in wild-type littermates, respectively. The levels of β-hydroxybutyrate, a product of

Table 1. *Comparison of cellularity in spleen and thymus and total blood cell counts in wild-type and bis-deficient mice*

	$bis^{+/+}$	$bis^{-/-}$
Splenocytes, $\times 10^6$	46.2±11.4 (7)	4.67±1.12 (12)*
Thymocytes, $\times 10^7$	16.7±2.79 (7)	2.97±0.87 (12)†
RBC, $\times 10^{12}$/l	6.18±0.18 (9)	6.77±0.16 (13)*
Platelets, $\times 10^9$/l	333±47.2 (9)	329±48.2 (13)
WBC, $\times 10^9$/l	6.63±0.63 (9)	2.76±0.34 (13)‡
Neutrophils	1.72±0.25 (9)	0.71±0.13 (13)†
Lymphocytes	3.98±0.32 (9)	1.63±0.17 (13)‡
Others	0.84±0.18 (9)	0.42±0.07 (13)*

Values are means ± SE for numbers of animals in parentheses. RBC, red blood cells; WBC, white blood cells; Others, monocytes, eosinophils, and basophils. *$P < 0.05$, †$P < 0.01$, ‡$P < 0.001$ compared with $bis^{+/+}$ littermates.

Table 2. *Profile of serum metabolites of wild-type and bis-deficient mice*

Parameter	$bis^{+/+}$	$bis^{-/-}$
Glucose, mg/dl	212.9±11.9 (13)	71.46±4.03 (17)‡
Insulin, pg/ml	768.5±119.7 (7)	282.9±77.5 (11)†
TAG, mg/dl	158.6±21.3 (7)	41.7±11.7 (7)‡
FFA, meq/l	1.2±0.2 (7)	1.0±0.2 (7)
Cholesterol, mg/dl	137.7±11.6 (7)	80.4±5.3 (7)‡
β-Hydroxybutyrate, mmol/l	2.80±0.56 (3)	6.44±1.30 (3)*

Results were obtained from mice at age 16 days and expressed as means ± SE for numbers of animals indicated in parentheses. TAG, triglyceride; FFA, free fatty acids. *$P < 0.05$, †$P < 0.01$, ‡$P < 0.001$ compared with wild-type littermates.

ketogenesis, were increased in $bis^{-/-}$ mice to ~2.5-fold above wild-type levels.

Although no obvious changes were observed by H & E staining (data not shown), Oil Red O staining revealed marked accumulation of lipids throughout the $bis^{-/-}$ liver tissues (Fig. 3*A*). Ultrastructural analysis of the hepatocytes of $bis^{-/-}$ mice revealed the presence of enlarged lipid particles and an increased number of lipid particles (Fig. 3*B*). The lipid contents of the $bis^{-/-}$ livers were analyzed to identify the type of accumulated lipids. In contrast to the serum profile of free fatty acids (FFA), which showed no difference between $bis^{-/-}$ and $bis^{+/+}$ mice, hepatic FFA levels in $bis^{-/-}$ livers were increased to twofold compared with wild-type littermates. $bis^{-/-}$ mice also had 2.8-fold and 3.4-fold increases in hepatic triglyceride and cholesterol levels, respectively, compared with control mice (Fig. 3*C*).

Quantitative RT-PCR revealed increased hepatic expression of mRNAs involved in gluconeogenesis in $bis^{-/-}$ mice, including glucose 6-phosphatase (G6Pase) and phosphoenolpyruvate carboxykinase (PEPCK) (Fig. 3*D*). The expression of several lipogenic genes, including fatty acid synthase (FAS) and stearoyl-CoA desaturase-1 (SCD-1), was markedly diminished, suggesting that de novo synthesis of fatty acids is inhibited in $bis^{-/-}$ mice (Fig. 3*D*). In addition, several hepatic genes involved in β-oxidation, such as carnitine palmitoyltransferase I (CPT-1) and medium-chain acyl-CoA dehydrogenase (MCAD), were induced in $bis^{-/-}$ mice (Fig. 3*D*). Thus hepatic steatosis in $bis^{-/-}$ mice is likely due to fatty acid delivery that exceeds the capacity for hepatic fatty acid oxidation to generate energy for gluconeogenesis, which are the typical metabolic changes in response to fasting (3, 8).

Bis deficiency caused no prominent apoptosis in diaphragm and cardiomyocytes. Bis is highly expressed in skeletal muscles (18), and a previous study with mice in which the *bis* gene had been disrupted by retroviral insertion described that, as the only abnormal finding, *bis*-deficient mice developed a fulminant myopathy characterized by noninflammatory myofibrillar degeneration with apoptotic features (10). However, in our model, no significant differences in H & E staining were found between the skeletal muscles from wild-type and *bis*-deficient mice (Fig. 4*A*), and the ventricular cardiomyocytes revealed similar frequencies in cells positive for TUNEL staining in wild-type and $bis^{-/-}$ mice (Fig. 4*B*). The diaphragm of $bis^{-/-}$ mice revealed a slight increase in TUNEL-positive apoptotic cells (Fig. 4*C*) but not as prominent as previously described by Homma et al. (10). When wild-type mice with body weight similar to $bis^{-/-}$ mice at day 12 after birth were fasted for 48 h, TUNEL-positive cells were increased in the diaphragm compared with feeding control (data not shown). Thus the increase of apoptotic cells in the diaphragm of $bis^{-/-}$ mice might represent a nutritionally insufficient status rather than acceleration of apoptosis due to the absence of Bis. Although no considerable abnormalities were noted in H & E staining, ultrastructures of muscles from *bis*-deficient mice exhibited discontinuous arrangement of myofibrils with thick and short Z bands but nuclei preserved normal morphology (Fig. 4*D*). Previous reports showed the colocalization of Bis with Z-disk proteins such as α-actinin and desmin (10). Thus Bis protein may contribute to preservation of the architecture of myofibrils, especially the integrity of Z bands, rather than the viability of myocytes.

DISCUSSION

Bis is expressed in various tissues, including skeletal muscle, heart, and kidney, and known to bind with several proteins, suggesting that it has diverse physiological functions. Using a *cre-loxP* system, we generated *bis* knockout mice and showed that these mice died within 3 wk after birth with metabolic derangements such as hypoglycemia and hepatic steatosis and significant reduction in the cellularity of the thymus and spleen. A previous study with mice in which the *bis* gene had been disrupted by retroviral insertion also reported premature death before weaning, although these mice died ~1 wk later than the time of death we observed (10). Furthermore, the previous study described severe degeneration and apoptosis in skeletal muscles and myocardium and no evidence of abnormality in other organs (10). In the present study, we found that the skeletal muscle fibers from $bis^{-/-}$ mice were irregular and smaller than those of wild-type littermates but found no evidence for massive apoptosis in the diaphragm, quadriceps, and cardiac muscles (Fig. 4 and data not shown). In addition, several of the phenotypes we report here, such as shrinkage of lymphoid organs and perturbations in metabolic homeostasis, were not observed in the previous report.

At present, the precise reasons for the differences in the phenotypes of our model and the previous model are not entirely clear. The method used for gene targeting may contribute to the different phenotypes observed. The previous *bis*-deficient model was developed with ES clones that had been mutagenized by retroviral insertion (10); our *bis*-deficient mice model was developed by precise deletion of exon 4 of the *bis* gene with a *Cre-loxP* system. Although the previous report does not describe which part of the *bis* gene was disrupted by retroviral insertion, partial disruption of the *bis* gene may have resulted in the expression of truncated Bis protein products, and these may have retained some function. In our system, we did not detect any full-length or truncated Bis protein by Western blotting using three kinds of antibodies raised against whole, COOH-terminal, and NH_2-terminal Bis peptides (Fig. 1 and Supplemental Fig. S1). However, the possibility that the sensitivity of immunoblotting was not high enough to detect a tiny amount of truncated Bis protein in our assay, as well as in the previous model, cannot be excluded. Another possible explanation for the discrepancy in the reported phenotypes of *bis*-deficient mice may be the extent of homogeneity in the genetic background. Diverse genetic backgrounds in hybrid

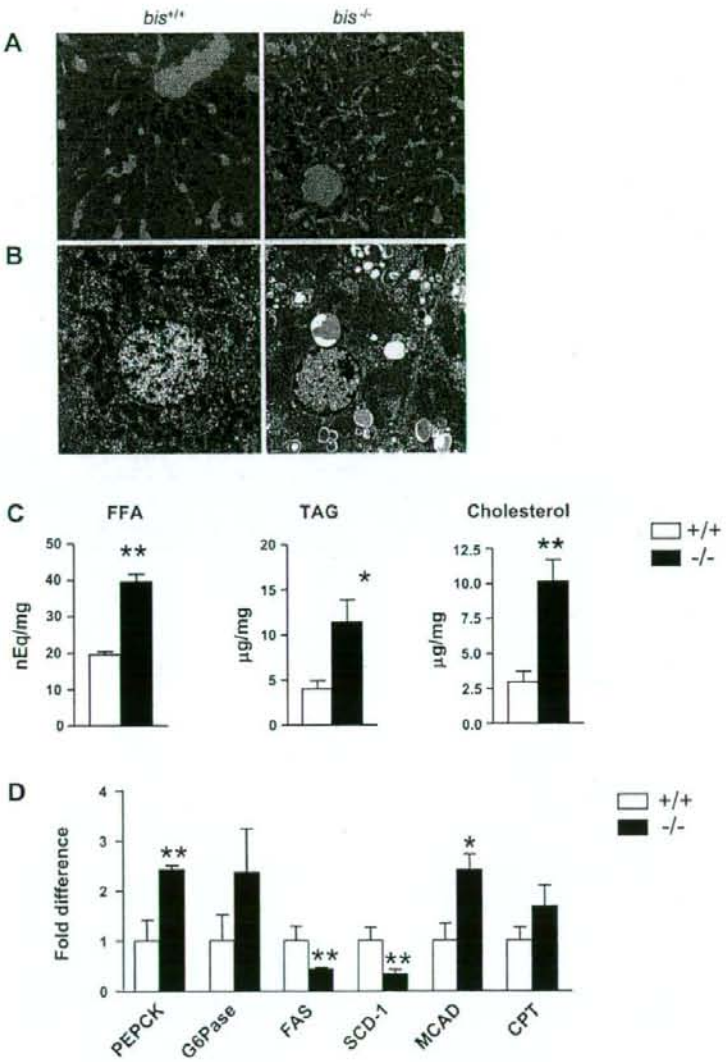

Fig. 3. Lipid accumulation in the liver of *bis*-deficient mice. *A*: Oil Red O staining of histological sections of liver from $bis^{+/+}$ and $bis^{-/-}$ mice. Red staining indicates neutral lipid accumulation. *B*: representative electron micrographs of $bis^{+/+}$ and $bis^{-/-}$ mice livers. Scale bars, 1 μm. *C*: increased levels of free fatty acid (FFA), triglyceride (TAG), and cholesterol in livers of $bis^{-/-}$ mice compared with livers of wild-type littermates. Results are expressed as means ± SE for 5 animals at 16 days of age. $*P < 0.05$, $**P < 0.01$, compared with wild-type littermates. *D*: alteration in mRNA levels of several genes involved in glucose or lipid metabolism in *bis*-deficient mice: quantitative RT-PCR of selected genes from livers of wild-type and *bis*-deficient mice. Data are means ± SE of 3 animals in each group, older than 15 days of age. Data are normalized relative to cyclophilin mRNA in the same samples, and wild-type values were arbitrarily set as 1.0. $*P < 0.05$, $**P < 0.01$, compared with wild-type littermates.

strains result in different degrees of compensatory responses, especially in response to metabolic challenges (2). For the generation of homozygous $bis^{-/-}$ mice we used heterozygous mice that were backcrossed with C57BL6 more than eight generations. Thus the effect of the Sv129 genetic background on the phenotypes of our study appeared insignificant. It is also possible that the metabolic disturbances observed in this study using biochemical and ultrastructure assays were not noticeable in the histological examinations performed by the previous research group.

The cause of death of the $bis^{-/-}$ mice was previously suggested to be respiratory failure, based on the marked degeneration of the diaphragm and intercostal muscle (10). It was also postulated that the decreased cardiac performance and subsequent pulmonary edema may have played a role in the death of the $bis^{-/-}$ mice (10). In the present study, massive apoptosis and degeneration of skeletal muscles were not observed in $bis^{-/-}$ mice (Fig. 4), suggesting that the loss of antiapoptotic activity in muscles is not the primary cause of death in these mice. Instead, the serious metabolic deterioration, such as sustained hypoglycemia and lipid accumulation in the liver, observed in our $bis^{-/-}$ mice model, may be ultimately responsible for the death of the animals.

What causes the perturbations in glucose and lipid metabolism in $bis^{-/-}$ mice? Analysis of the hepatic expression of key enzymes in the pathways of glucose and lipid metabolism

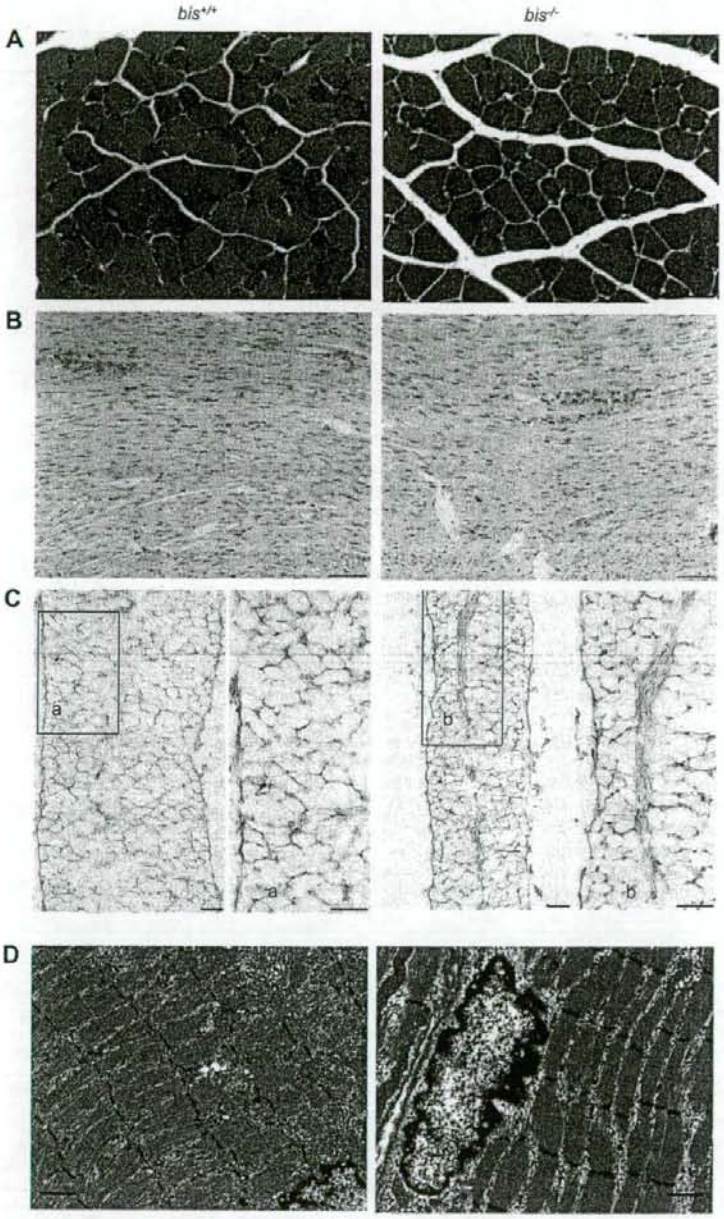

Fig. 4. No massive apoptotic features in myocytes of *bis*-deficient mice. *A*: hematoxylin and eosin staining of quadriceps femoris muscles of wild-type and *bis*-deficient mice. Scale bars, 30 μm. *B* and *C*: TUNEL staining of ventricle (*B*) and thin sections of diaphragm (*C*) of wild-type and $bis^{-/-}$ mice. *C*, *a* and *b*: Higher magnifications of boxed areas. Scale bars, 50 μm. *D*: transelectron microscopy of quadriceps femoris muscles of wild-type and *bis*-deficient mice. Scale bars, 1 μm.

revealed an increase in gluconeogenesis and lipolysis and a decrease in lipogenesis in $bis^{-/-}$ mice (Fig. 3*D*). These changes, which were also accompanied by a decrease in peripheral fat and serum triglyceride levels (Table 2), are typical of the adaptive response to a scarcity of glucose in serum that supplies the energy for gluconeogenesis in the liver, which is observed after fasting (35). Since we frequently observed that, even throughout their weight loss, $bis^{-/-}$ mice were trying to suckle, it is unlikely that isolation from the feeding mother or loss of appetite was the cause of their hypoglycemia. An impediment in the uptake or absorption of milk possibly caused delayed growth, due to an insufficiency

of nutrients for normal growth, and substantially metabolic deterioration, the same results of fasting. Since the amounts of milk in the stomachs of $bis^{-/-}$ mice were low at ≥16 days of age and no obvious histological abnormalities were found in the intestines of $bis^{-/-}$ mice (Supplemental Fig. S2), the ingestion of milk, rather than the process of absorption, appears to be impaired in $bis^{-/-}$ mice. The hypothesis that hypophagia or dysphagia is linked to nutritional problems and growth retardation in $bis^{-/-}$ mice is supported by a previous mutation study of *starvin* (*stv*), a *Drosophila* gene encoding a Bag-domain protein (6). The Bag domain is located in the COOH terminal of Bis, shared with several proteins comprising the Bag family (33). Coulson et al. (6) showed that mutation of *stv* results in a failure of larvae to grow after hatching and a severely impaired ability to take up food. The expression of STV was shown to be highly specific in embryonic somatic muscle and tendon cells, suggesting a role in muscle development or function. However, the gross morphology and function of somatic muscles including mouth-hook movement is predominantly normal in *stv* mutants, indicating that the feeding disability of *stv* mutants is not linked to dysfunction of skeletal muscles. Thus, in light of the study of *stv* mutants of *Drosophila*, the malnutrition status observed in *bis* deficiency is associated with impairment in uptake of milk, which is probably not caused by dysfunction of skeletal muscles. However, although obvious apoptotic changes were not found in the skeletal muscles in $bis^{-/-}$ mice, it is possible that Bis deletion caused functional weakness of muscles involved in suckling or swallowing or abnormal esophageal motor function shown in achalasia, a esophageal motility disorder in humans (16). Therefore, the role of Bis in the physiological regulation of swallowing remains to be elucidated.

We also observed a dramatic involution of the thymus and spleen in mice with a homozygous *bis* gene deletion (Fig. 2, *C* and *D*). At present, the direct link between the two representative phenotypes of $bis^{-/-}$ mice, metabolic deterioration and involution of the thymus and spleen, remains unclear. The thymus has been shown to be significantly affected in malnutrition, undergoing a severe atrophy due to apoptosis-induced thymocyte depletion (22, 24, 30). We showed that the reduction in the relative weight of the thymus and spleen was not obvious until 12 days after birth (Fig. 2*E*), at a time when body weight was still increasing and the serum glucose level was within the normal range (Fig. 2*A* and data not shown). Thus the involution of the thymus and spleen appears to be directly or indirectly linked to the nutritional status of $bis^{-/-}$ mice. Shrinkage of the thymus and spleen has also been described in *bcl-2*-deficient mice (13, 36). Since Bis binds Bcl-2 (18), interaction between Bis and Bcl-2 may be required for normal physiology of these lymphoid organs. However, $bcl\text{-}2^{-/-}$ mice have selective lymphopenia, but $bis^{-/-}$ mice have an overall decrease in white blood cells (Table 1). Furthermore, thymic and hepatic levels of Bcl-2 and HSP70, another Bis binding partner (33), were not decreased in protein extracts from *bis*-deficient mice in a Western blot analysis (data not shown). Thus the phenotypes observed in $bis^{-/-}$ mice are not mainly due to the disruption of the interaction between Bis and Bcl-2, or HSP70, but due to the specific effect of ablation of *bis* gene.

Bis has been shown to be highly expressed in lymphocytic leukemia cells, and downmodulation of Bis increases susceptibility to apoptosis in normal and neoplastic leukocytes (26–28). Therefore, our results showing significant decrease in leukocytes in peripheral blood cells from $bis^{-/-}$ mice support the previous reports for survival-sustaining roles of Bis in leukocytes. However, it is not certain whether the absence of Bis affects the viability of peripheral leukocytes or the function of progenitor cells in bone marrow. Thus, with the shrinkage of lymphoid organs, the decreases in the leukocyte numbers in $bis^{-/-}$ mice suggest the expanded roles of Bis in the physiology of hematopoietic cells and in the development of lymphoid organs, not confined to prosurvival activity of lymphocytes.

In this study, we generated *bis*-deficient mice and demonstrated that *bis* ablation resulted in growth retardation and early lethality with serious metabolic deterioration and involution of the thymus and spleen. Our results suggest that Bis is critical for postnatal growth and survival. However, the critical role for Bis in the regulation of feeding and the physiology of the thymus and spleen, which may or may not be linked, remains to be fully defined.

ACKNOWLEDGMENTS

We thank Y. Maruyama and A. Kawai for technical assistances and I. H. Oh and J. Kim for helpful discussions.

GRANTS

This work was partly supported by a Korea Research Foundation Grant funded by the Korean government (MOEHRD) (KRF-2004-041-E00043), a Korea Science and Engineering Foundation (KOSEF) grant funded by the Korean government (MOST) (R01-2006-000-10208-0), grants for Scientific Research from the Ministry of Education, Science, Sports and Culture, and a grant for Research on Dementia and Bone Fracture from the Ministry of Health, Labor and Welfare, Japan.

REFERENCES

1. **Bonelli P, Petrella A, Rosati A, Romano MF, Lerose R, Pagliuca MG, Amelio T, Festa M, Martire G, Venuta S, Turco MC, Leone A.** BAG3 protein regulates stress-induced apoptosis in normal and neoplastic leukocytes. *Leukemia* 18: 358–360, 2004.
2. **Burgess SC, Jeffrey FM, Storey C, Milde A, Hausler N, Merritt ME, Mulder H, Holm C, Sherry AD, Malloy CR.** Effect of murine strain on metabolic pathways of glucose production after brief or prolonged fasting. *Am J Physiol Endocrinol Metab* 289: E53–E61, 2005.
3. **Chakravarthy MV, Pan Z, Zhu Y, Tordjman K, Schneider JG, Coleman T, Turk J, Semenkovich CF.** "New" hepatic fat activates PPARalpha to maintain glucose, lipid, and cholesterol homeostasis. *Cell Metab* 1: 309–322, 2005.
4. **Chen L, Wu W, Dentchev T, Zeng Y, Wang J, Tsui I, Tobias JW, Bennett J, Baldwin D, Dunaief JL.** Light damage induced changes in mouse retinal gene expression. *Exp Eye Res* 79: 239–247, 2004.
5. **Chiappetta G, Ammirante M, Basile A, Rosati A, Festa M, Monaco M, Vuttariello E, Pasquinelli R, Arra C, Zerilli M, Todaro M, Stassi G, Pezzullo L, Gentilella A, Tosco A, Pascale M, Marzullo L, Belisario MA, Turco MC, Leone A.** The antiapoptotic protein BAG3 is expressed in thyroid carcinomas and modulates apoptosis mediated by tumor necrosis factor-related apoptosis-inducing ligand. *J Clin Endocrinol Metab* 92: 1159–1163, 2007.
6. **Coulson M, Robert S, Saint R.** *Drosophila* starvin encodes a tissue-specific BAG-domain protein required for larval food uptake. *Genetics* 171: 1799–1812, 2005.
7. **Doong H, Price J, Kim YS, Gasbarre C, Probst J, Liotta LA, Blanchette J, Rizzo K, Kohn E.** CAIR-1/BAG-3 forms an EGF-regulated ternary complex with phospholipase C-gamma and Hsp70/Hsc70. *Oncogene* 19: 4385–4395, 2000.
8. **Finck BN, Gropler MC, Chen Z, Leone TC, Croce MA, Harris TE, Lawrence JC Jr, Kelly DP.** Lipin 1 is an inducible amplifier of the hepatic PGC-1alpha/PPARalpha regulatory pathway. *Cell Metab* 4: 199–210, 2006.
9. **Foretz M, Ancellin N, Andreelli F, Saintillan Y, Grondin P, Kahn A, Thorens B, Vaulont S, Viollet B.** Short-term overexpression of a consti-

tutively active form of AMP-activated protein kinase in the liver leads to mild hypoglycemia and fatty liver. *Diabetes* 54: 1331–1339, 2005.
10. **Homma S, Iwasaki M, Shelton GD, Engvall E, Reed JC, Takayama S.** BAG3 deficiency results in fulminant myopathy and early lethality. *Am J Pathol* 169: 761–773, 2006.
11. **Inoue N, Ikawa M, Isotani A, Okabe M.** The immunoglobulin superfamily protein Izumo is required for sperm to fuse with eggs. *Nature* 434: 234–238, 2005.
12. **Iwasaki M, Homma S, Hishiya A, Dolezal SJ, Reed JC, Takayama S.** BAG3 regulates motility and adhesion of epithelial cancer cells. *Cancer Res* 67: 10252–10259, 2007.
13. **Kamada S, Shimono A, Shinto Y, Tsujimura T, Takahashi T, Noda T, Kitamura Y, Kondoh H, Tsujimoto Y.** bcl-2 deficiency in mice leads to pleiotropic abnormalities: accelerated lymphoid cell death in thymus and spleen, polycystic kidney, hair hypopigmentation, and distorted small intestine. *Cancer Res* 55: 354–359, 1995.
14. **Kassis JN, Guancial EA, Doong H, Virador V, Kohn EC.** CAIR-1/BAG-3 modulates cell adhesion and migration by downregulating activity of focal adhesion proteins. *Exp Cell Res* 312: 2962–2971, 2006.
15. **Kyratsous CA, Silverstein SJ.** BAG3, a host cochaperone, facilitates varicella-zoster virus replication. *J Virol* 81: 7491–7503, 2007.
16. **Lacy BE, Weiser K.** Esophageal motility disorders: medical therapy. *J Clin Gastroenterol* 42: 652–658, 2008.
17. **Lee JH, Jeon MH, Seo YJ, Lee YJ, Ko JH, Tsujimoto Y, Lee JH.** CA repeats in the 3′-untranslated region of bcl-2 mRNA mediate constitutive decay of bcl-2 mRNA. *J Biol Chem* 279: 42758–42764, 2004.
18. **Lee JH, Takahashi T, Yasuhara N, Inazawa J, Kamada S, Tsujimoto Y.** Bis, a Bcl-2-binding protein that synergizes with Bcl-2 in preventing cell death. *Oncogene* 18: 6183–6190, 1999.
19. **Lee MY, Kim SY, Choi JS, Choi YS, Jeon MH, Lee JH, Kim IK, Lee JH.** Induction of Bis, a Bcl-2-binding protein, in reactive astrocytes of the rat hippocampus following kainic acid-induced seizure. *Exp Mol Med* 34: 167–171, 2002.
20. **Lee MY, Kim SY, Shin SL, Choi YS, Lee JH, Tsujimoto Y, Lee JH.** Reactive astrocytes express bis, a bcl-2-binding protein, after transient forebrain ischemia. *Exp Neurol* 175: 338–346, 2002.
21. **Liao Q, Ozawa F, Friess H, Zimmermann A, Takayama S, Reed JC, Kleeff J, Buchler MW.** The anti-apoptotic protein BAG-3 is overexpressed in pancreatic cancer and induced by heat stress in pancreatic cancer cell lines. *FEBS Lett* 503: 151–157, 2001.
22. **Morishita S, Sato EF, Takahashi K, Manabe M, Inoue M.** Insulin-induced hypoglycemia elicits thymocyte apoptosis in the rat. *Diabetes Res Clin Pract* 40: 1–7, 1998.
23. **Pagliuca MG, Lerose R, Cigliano S, Leone A.** Regulation by heavy metals and temperature of the human BAG-3 gene, a modulator of Hsp70 activity. *FEBS Lett* 541: 11–15, 2003.
24. **Prentice AM.** The thymus: a barometer of malnutrition. *Br J Nutr* 81: 345–347, 1999.
25. **Proctor G, Jiang T, Iwahashi M, Wang Z, Li J, Levi M.** Regulation of renal fatty acid and cholesterol metabolism, inflammation, and fibrosis in Akita and OVE26 mice with type 1 diabetes. *Diabetes* 55: 2502–2509, 2006.
26. **Romano MF, Festa M, Pagliuca G, Lerose R, Bisogni R, Chiurazzi F, Storti G, Volpe S, Venuta S, Turco MC, Leone A.** BAG3 protein controls B-chronic lymphocytic leukaemia cell apoptosis. *Cell Death Differ* 10: 383–385, 2003.
27. **Romano MF, Festa M, Petrella A, Rosati A, Pascale M, Bisogni R, Poggi V, Kohn EC, Venuta S, Turco MC, Leone A.** BAG3 protein regulates cell survival in childhood acute lymphoblastic leukemia cells. *Cancer Biol Ther* 2: 508–510, 2003.
28. **Rosati A, Ammirante M, Gentilella A, Basile A, Festa M, Pascale M, Marzullo L, Belisario MA, Tosco A, Franceschelli S, Moltedo O, Pagliuca G, Lerose R, Turco MC.** Apoptosis inhibition in cancer cells: a novel molecular pathway that involves BAG3 protein. *Int J Biochem Cell Biol* 39: 1337–1342, 2007.
29. **Rosati A, Leone A, Del Valle L, Amini S, Khalili K, Turco MC.** Evidence for BAG3 modulation of HIV-1 gene transcription. *J Cell Physiol* 210: 676–683, 2007.
30. **Savino W, Dardenne M, Velloso LA, Dayse Silva-Barbosa S.** The thymus is a common target in malnutrition and infection. *Br J Nutr* 98, *Suppl* 1: S11–S16, 2007.
31. **Schwarz DA, Barry G, Mackay KB, Manu F, Naeve GS, Vana AM, Verge G, Conlon PJ, Foster AC, Maki RA.** Identification of differentially expressed genes induced by transient ischemic stroke. *Brain Res Mol Brain Res* 101: 12–22, 2002.
32. **Seo YJ, Jeon MH, Lee JH, Lee YJ, Youn HJ, Ko JH, Lee JH.** Bis induces growth inhibition and differentiation of HL-60 cells via up-regulation of p27. *Exp Mol Med* 37: 624–630, 2005.
33. **Takayama S, Xie Z, Reed JC.** An evolutionarily conserved family of Hsp70/Hsc70 molecular chaperone regulators. *J Biol Chem* 274: 781–786, 1999.
34. **Tanaka N, Moriya K, Kiyosawa K, Koike K, Gonzalez FJ, Aoyama T.** PPARalpha activation is essential for HCV core protein-induced hepatic steatosis and hepatocellular carcinoma in mice. *J Clin Invest* 118: 683–694, 2008.
35. **Teusink B, Voshol PJ, Dahlmans VE, Rensen PC, Pijl H, Romijn JA, Havekes LM.** Contribution of fatty acids released from lipolysis of plasma triglycerides to total plasma fatty acid flux and tissue-specific fatty acid uptake. *Diabetes* 52: 614–620, 2003.
36. **Veis DJ, Sorenson CM, Shutter JR, Korsmeyer SJ.** Bcl-2-deficient mice demonstrate fulminant lymphoid apoptosis, polycystic kidneys, and hypopigmented hair. *Cell* 75: 229–240, 1993.